Available online at www.HEFJournal.org

ISSN: 2785-2997

Journal of
Human, Earth, and Future

Vol. 6, No. 2, June, 2025

Integrating Satellite and UAV Imagery for Mangrove Aboveground Biomass and Carbon Stock Modeling

Sinlapachat Pungpa [1], Krisanadej Jaroensutasinee [2*], Mullica Jaroensutasinee [2], Wacharapong Srisang [3], Sirilak Chumkiew [1*], Elena B. Sparrow [4]

[1] *School of Biology, Institute of Science, Suranaree University of Technology, Muang Nakhon Ratchasima, 30000, Thailand.*

[2] *Center of Excellence for Ecoinformatics, Walailak University, Nakhon Si Thammarat, 80160, Thailand.*

[3] *Faculty of Science and Agricultural Technology, Rajamangala University of Technology Lanna, 52000, Lampang, Thailand.*

[4] *Department of Natural Resources and Environment, University of Alaska Fairbanks, AK, United States.*

Received 26 March 2025; Revised 11 May 2025; Accepted 17 May 2025; Published 01 June 2025

Abstract

This study aimed to: (1) quantify aboveground biomass (AGB) and carbon (AGC) stocks in the Banlaem mangrove forest, Nakhon Si Thammarat, Thailand; and (2) construct an AGB estimation model using vegetation indices (VIs) derived from Sentinel-2, Landsat-8, and unmanned aerial vehicle (UAV) imagery. On-the-ground measurements were carried out to evaluate the AGB and AGC stocks of the mangrove forest. VIs were then calculated using passive remote sensing data, including satellite and UAV imagery. These indices were compared through multiple regression analysis with the ground-truthed AGB for evaluation. Three mangrove species were found: *Rhizophora mucronata*, *R. apiculata*, and *Avicennia Marina*. Overall, the AGB and AGC stocks ranged from 0 to 179.78 tons•ha^{1} (56.30 ± 51.81 tons•ha^{1}) and 0 to 89.89 tons•ha^{1} (28.15 ± 25.90 tons•ha^{1}), respectively. The best AGB model exhibited an R^2 of 0.73 and an *RMSE* of 22.0 tons•ha^{1}. This study presents a novel approach for estimating AGB and AGC stocks in the Thai mangrove ecosystem by integrating a UAV with two open-access satellite imagery sources. Combining multiple VIs (NDVI, SAVI, and GNDVI) with CHM provides better accuracy for the mangrove AGB estimation model than using a single variable.

Keywords: Aboveground Biomass; Carbon Stock; Mangrove; Remote Sensing; Vegetation Index.

1. Introduction

Blue carbon ecosystems play a vital role in capturing and storing carbon, supporting coastal and marine biodiversity, and acting as natural barriers against shoreline erosion, severe weather, pollution, and rising sea levels [1]. Among these, mangroves stand out due to their exceptional ability to store carbon over long periods and contribute significantly to lowering greenhouse gas concentrations and atmospheric CO_2 [1]. They are also the most comprehensively studied in terms of carbon dynamics, with estimates indicating that globally, mangrove ecosystems sequester around 700 million tons of carbon annually via gross primary production [2]. Their high rate of carbon absorption through photosynthesis underscores their importance in mitigating climate change, highlighting the need for consistent monitoring [3].

* Corresponding author: krisanadej@gmail.com; s.chumkiew@g.sut.ac.th

http://dx.doi.org/10.28991/HEF-2025-06-02-014

Sustainable management of mangrove blue carbon relies on the effective measurement, mapping, and monitoring of mangrove forests [4]. Few studies have focused on their carbon estimation, primarily due to challenges associated with technical limitations and the shortcomings of traditional methods. These challenges include financial, work crews, time consumption, and data inventory processing constraints [5]. In addition, due to the challenging accessibility of mangrove habitats, most studies are confined to small areas and rely on a limited number of field samples [6]. These constraints underscore the need for improved methods to assess mangrove carbon.

Remote sensing (RS) provides methods for accurately estimating carbon in mangrove forests, thereby eliminating the difficulties associated with conventional techniques. Conventional methods depend solely on field surveys for estimation, with their effectiveness restricted to small-scale areas [7]. In contrast, remotely sensed research studies offer a way to overcome the challenges of conducting fieldwork, mainly through passive RS, which is cost-effective and easy to interpret while providing a wealth of information [8]. Satellite-based research is becoming increasingly widespread due to the growing accessibility of satellite data, improved image resolution, time-series datasets, and reduced time and computational costs [9]. However, unmanned aerial vehicles (UAVs) can carry multiple sensors, enabling the collection of diverse data types at varying resolutions [10]. VIs can show a strong correlation with mangrove aboveground biomass (AGB), as demonstrated by models achieving R^2 values of 0.81 using Sentinel-2 [11] and 0.90 using Landsat-8 [5]. Developing RS approaches is necessary for estimating mangrove biomass, particularly in large-scale areas and inaccessible areas.

Between 1989 and 2020, the Lower Mekong Region (LMR), which includes Myanmar, Thailand, Cambodia, and Vietnam, saw a dramatic increase in mangrove area. During this time period, Thailand, a Southeast Asian country, became a significant contributor to the region's mangrove forest wealth by substantially increasing mangrove cover from 339,613 ha to 601,642 ha [12]. To date, only one study has utilized remote sensing techniques to estimate mangrove carbon stocks in Thailand. Specifically, GeoEye-1 imagery and ASTER GDEM data were employed to assess mangrove carbon along the Andaman Coast [13]. The majority of research in Thailand has relied on conventional field-based approaches for estimating mangrove carbon storage [14, 15]. In Nakhon Si Thammarat, for instance, traditional measurement methods have also been employed [16]. In contrast, studies across Southeast Asia have demonstrated the efficacy of remote sensing for estimating mangrove carbon [7, 17-19]. These findings underscore the need to develop advanced methods for estimating mangrove carbon in Thailand, a country experiencing a rise in mangrove cover.

The Banlaem mangrove forest, situated in the Banlaem community of Nakhon Si Thammarat, southern Thailand, is a promising carbon sink that warrants careful consideration. From the personal interview with the community tourism coordinator in the community, the area experienced an ecological shift from a sandy beach to a muddy soil wetland approximately 30 to 40 years ago (1984–1994); following this change, several diverse mangrove planting initiatives have been carried out by the introduction of loop-root mangroves (*Rhizophora mucronata*), which promoted the rapid expansion of the mangrove ecosystem. However, regarding carbon assessment efforts, this community lacks quantitative data on carbon storage, which would be important in impact assessments and monitoring efforts in this mangrove area.

To fill the gaps, this work aimed to (1) assess AGB and AGC stock in the Banlaem mangrove forest, Nakhon Si Thammarat, Thailand, and (2) develop models using VIs from satellites (Sentinel-2, Landsat-8) and a UAV to investigate both AGB and AGC stock. Moreover, this study is the first to examine the biodiversity in the Banleam mangrove forest. We conducted the ground truth assessment to establish the baseline AGB and AGC stock for validation against the RS data. A model for estimating biomass and carbon was developed using regression analysis. The findings provide a tool for estimating carbon storage in the Banlaem mangrove forest, enabling land managers to make informed decisions about harvesting, tree planting, and habitat preservation in this area, thereby promoting community engagement in sustainable management and carbon offset projects.

2. Material and Methods

2.1. Methodology

The details of the study's methodology are shown in Figure 1. We collected data from both ground measurements and remote sensing (RS) sources. We recorded information regarding mangrove trees and their biodiversity indices factor. RS data, including Landsat-8, Sentinel-2, and UAV imagery, were processed to generate vegetation indices (VIs) and a canopy height model (CHM), which were then used in regression analysis to develop mangrove AGB models. Finally, statistical methods were employed to evaluate the performance of the models.

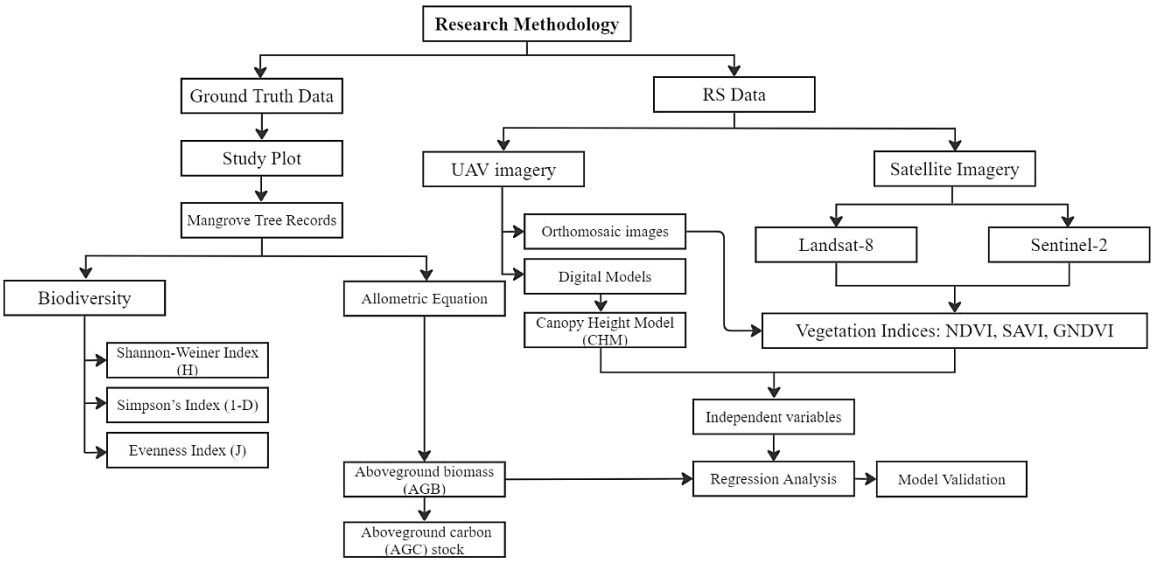

Figure 1. Methodology of this study

2.2. Study Site

The Banlaem mangrove forest (8°36'32.7" N, 99°57'59.0" E) is geographically located in the Banlaem community, Nakhon Si Thammarat Province, Southern Thailand, in a tropical region (Figure 2). The entire study site covers 123.5 ha, designated as an ecotourism zone. The *R. mucronata* is the only species intentionally planted in the Banlaem mangrove forest. To grow, propagules from *R. mucronata* are placed in muddy soil, with each propagule spaced 1.0-1.5 m apart and inserted to a depth of 15-20 cm. However, observations in this study indicated that another species (*A. marina*) dominates the upland areas as an interior species, while *R. mucronata* primarily occupies the peripheral zones (edge species). In Southern Thailand, the average annual rainfall ranges from 1,200 to 4,500 mm, with higher amounts recorded on the windward side compared to the leeward side. The mean temperature is 27.5°C [20].

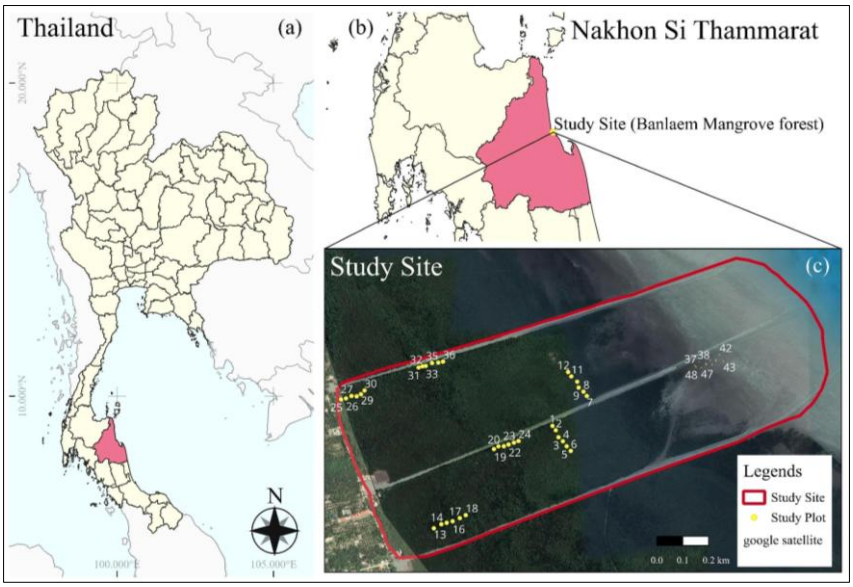

Figure 2. Study area: (a) Thailand map, (b) Nakhon Si Thammarat province, Southern Thailand, and (c) study plots arrangements in the study site (Banlaem mangrove forest)

2.3. Ground Truth Data Collection

Line transect plot configurations were established to assess the AGB and AGC stocks within the Banlaem mangrove forest, for the study period of April 2023 to July 2024. The study plot design followed Kauffman and Donato's protocol [21]. Six circular plots (7 m radius) per line transect yielded 36 total plots (plots 1–36). Additionally, square plots (1 × 1 m²) were established for mangrove seedling assessments, designated as plots 37–48. In total, 48 sampling plots were used in the study (Figure 2a-b). The location and dimensions of the studied plots were restricted due to the challenges of accessing the mangrove areas. At each plot, data on mangrove tree scientific names, DBH (≥5 cm [22]), tree density, and basal area (BA) were determined. Species were identified using a handbook [23]

and expert consultation. Unique tree codes and all data were documented on collection forms. A species-specific allometric equation, Equation 1, was applied [24] to estimate the AGB. A wood density (ρ) was derived from the Global Wood Density Database [25].

$$AGB\ (kg) = 0.25 \times \rho\ (g/cm^3) \times DBH^{2.46} \quad (1)$$

where: DBH (cm) at 0.3 m above prop roots (Rhizophoraceae). The AGC stock is estimated to be 50 percent of the biomass [26]. Understory vegetation, seedlings, and herb carbon were not included in the analysis due to their minimal contribution to mangrove ecosystem carbon storage [21, 27].

Furthermore, this study calculated the diversity indices for the mangrove tree species in the Banlaem mangrove forest. Biodiversity was measured using the Shannon-Weiner Index (H) and Simpson's Index (1-D). The value of H varies among sampling plots and is influenced by species richness (S). The Evenness Index (J) was utilized to measure species dominance. Equations 2, 3, and 4 illustrate the calculations for H, D, and J, respectively [28, 29].

$$H = -\sum_{i=1}^{S} p_i \times ln\ ln\ p_i \quad (2)$$

where p_i represents the proportion of individuals of species i, and ln denotes the natural logarithm. The value of H varies between 0 and H_{max}. A higher H value indicates greater diversity.

$$D = \sum_{i=1}^{s} (\frac{n_i}{N})^2 \quad (3)$$

where n_i is the count of individuals of species i, and N is the total individual count, 1-D ranges from 0 to 1. A value of 1 indicates maximum diversity, and 0 means no diversity.

$$J = \frac{H}{H_{max}} \quad (4)$$

The value of J varies between 0 and 1. A low J value indicates that one or a few species dominate the study plots.

2.4. Remote Sensing Data Collection

This study utilized data from two open-access satellites, Sentinel-2 and Landsat-8 (Table 1). Sentinel-2B Level 2A imagery (MSI, atmospherically corrected surface reflectance) was downloaded from the ESA's Sentinel Scientific Data Hub. Landsat-8 Collection 2 Level 2 imagery (atmospherically corrected surface reflectance) was downloaded from the United States Geological Survey (USGS). Images were selected based on minimal cloud cover (Landsat-8: 3.16%, Sentinel-2: 5.65%) and their temporal closeness to the ground data collection dates.

The study also incorporated UAV imagery captured using a DJI Mavic 2 Enterprise Advanced, equipped with visible and near-infrared (Vis/NIR) cameras. UAV imagery was captured during ground truth data collection (on 28th April 2023 and 15th July 2024). The frontal overlap, side lap, and flight height were set to 80%, 70%, and 90 m, respectively. The spatial resolution (GSD) was 1.48 cm/pixel. The UAV imagery was processed in Pix4Dmapper (version 4.8.4) to produce an orthomosaic image, a digital terrain model (DTM), and a digital surface model (DSM). The imagery was calibrated using Pix4D photogrammetric processing, which optimized both internal and external camera parameters. Canopy Height Model (CHM) was generated in QGIS using photogrammetry-derived data by subtracting the DTM from the DSM. This value represents the measured vegetation height above the ground [30]. This calculation was performed using the raster calculation tool in Quantum GIS (version 3.34.1-Prizren). In addition to VIs, this study included the CHM from the UAV as an additional variable for developing the AGB model in the Banlaem mangrove forest.

Table 1. Landsat-8 and Sentinel-2 Satellite image codes, date, and resolution

No.	Image Codes	Date	Resolution (m)	Remarks
1	LC08_L2SP_129054_20230331_20230405_02_T1_SR_B3	31/03/2023	30	Landsat-8
2	LC08_L2SP_129054_20230331_20230405_02_T1_SR_B4	31/03/2023	30	Landsat-8
3	LC08_L2SP_129054_20230331_20230405_02_T1_SR_B5	31/03/2023	30	Landsat-8
4	S2B_MSIL2A_20230312T033539_N0509_R061_T47PPK__B03_10m	12/03/2023	10	Sentinel-2
5	S2B_MSIL2A_20230312T033539_N0509_R061_T47PPK__B04_10m	12/03/2023	10	Sentinel-2
6	S2B_MSIL2A_20230312T033539_N0509_R061_T47PPK__B08_10m	12/03/2023	10	Sentinel-2

2.5. Vegetation Index Calculation

To develop aboveground biomass (AGB) models for the Banlaem mangrove forest (Table 2), three vegetation indices (VIs) were calculated using the raster calculation tool in Quantum GIS (version 3.34.1-Prizren). The resulting VIs were subsequently integrated with ground-truth AGB, which was derived from allometric equations, to construct the AGB estimation model.

Table 2. The equations of the VIs used for the development of the mangrove AGB model

No.	Vegetation Indices	Equations		References
1	NDVI (normalized difference vegetation index)	$NDVI = \left(\frac{NIR - RED}{NIR + RED}\right)$	(5)	[31]
2	SAVI (soil-adjusted vegetation index)	$SAVI = \left(\frac{NIR - RED}{NIR + RED + L}\right) \times (L + 1)$	(6)	[32]
3	GNDVI (green normalized difference vegetation index)	$GNDVI = \left(\frac{NIR - GREEN}{NIR + GREEN}\right)$	(7)	[33]

Where: L – soil brightness correction factor (0.5), GREEN – green wavelength, RED – red wavelength, NIR – near-infrared wavelength

2.6. AGB Model Development and Validation

Linear and multiple linear regression models were analyzed and developed to predict mangrove AGB using Jamovi 2.6.2. The ground AGB was used as the dependent variable, while NDVI, SAVI, GNDVI, and CHM were considered independent variables for estimating AGB in the Banlaem mangrove forest. The most accurate models were validated based on the correlation coefficient (*R*), coefficient of determination (R^2), probability value (*p-value*), root mean square error (*RMSE*), and residual plots. However, this study excluded specific plots (plots 13-18) from the AGB model development due to the UAV's inaccessibility to those areas. Mangrove seedling plots (37–48) were excluded from the regression analysis due to distinct linear patterns in their residuals and differing plot sizes relative to the other plots, which exhibited random patterns indicating a good model fit to the linear model. Additionally, their varying plot sizes may have introduced variability in the independent variables, leading to their exclusion as outliers.

3. Results

3.1. Ground Truth Records, Biodiversity, and Carbon Stock

We made ground observations and measurements from April 2023 to July 2024 in the Banlaem mangrove forest, Nakhon Si Thammarat, Thailand. Species occurrences, tree records (including density, DBH, and BA), and biodiversity indices are presented in Table 3. Regarding the species occurrence, we found only a few species in this study area. These included mangrove trees from the family Rhizophoraceae, genus *Rhizophora* (*R. mucronata* and *R. apiculata*), and the family Acanthaceae, genus *Avicennia* (*A. marina*), totalling three species (Figure 3 a-c). *A. marina* was the dominant species, which can be found in every plot (for mature mangroves). We categorized the mangrove trees into three distinct composition types: (1) a mixture of grey mangrove (*A. marina*) and loop-root mangroves (*Rhizophora* spp.), observed in plots 1, 2, 7, 13–22, and 31–36; (2) *A. marina*, found in plots 3–6, 8–12, and 23–30; and (3) predominantly seedlings, with *R. mucronata* being dominant in plots 37–48. The overall density was 4,386±4,732 mangrove trees · ha^{-1} with the mean DBH and BA of 6.32±3.84 cm and 8.76±7.40 m^2 · ha^{-1}, respectively. In general, the *Rhizophora* spp. appeared to function as edge species, predominantly distributed along the boundaries of upland areas, whereas *A. marina* was more commonly found in the interior. However, within the study plots, *Rhizophora* spp. frequently co-occurred with *A. marina*. *Rhizophora* spp. and did not occur alone, except in the small-mangrove (seedlings) plot group. In contrast, some plots consisted solely of *A. marina*.

(a) (b) (c)

Figure 3. The mangrove tree species found in the study area include (a) *Rhizophora apiculata*, (b) *Rhizophora mucronata*, and (c) *Avicennia marina*

The mangrove tree data showed that seedlings had a higher tree density than mature trees. The overall density of mature trees was 1,959±1,034.31 mangrove trees · ha^{-1}. The density varied depending on the composition of mangrove

tree species. In contrast, seedlings had an overall density of 11,667±3,892.49 mangrove trees · ha^{-1}, which was higher than that of the mature trees. The mean DBH and BA in the mature tree were 8.43±1.23 cm and 11.68±6.20 m^2 · ha^{-1}, respectively. Seedlings had a height of less than 1.30 m, resulting in the mean DBH and BA of 0 cm and 0 m^2 · ha^{-1}, respectively. This study also revealed aspects of biodiversity in the Banlaem mangrove forest. The species richness in the Banlaem mangrove forest was three. Overall, the biodiversity indices indicated the limited biodiversity in this area. For the mature mangrove trees, the 1-D index was 0.15±0.18, indicating that the presence of dominant species resulted in limited species diversity. The H index was 0.23±0.27, indicating that only a small number of species were found. The J index was 0.33 ± 0.38, indicating low species evenness within the community. However, for the seedlings, all indices had a value of 0 because only a single species was found in each plot.

The AGB and AGC stocks in the Banlaem mangrove ecosystem varied across the study plots (Figure 4). Overall, the AGB and AGC stocks ranged from 0 to 179.78 (56.30±51.81) and 0 to 89.89 (28.15±25.90) ton · ha^{-1}, respectively. Mature mangroves (plots 1–36) had higher AGB and AGC stocks compared to the seedlings (plots 37–48). The highest AGC stock was recorded in the plot with the largest mean DBH (plot 16, DBH = 11.62±2.52 cm), where *A. marina* and *R. mucronata* coexisted. In contrast, the mangrove seedlings along the seafront had a DBH ≤5 cm, which was considered negligible in terms of carbon stock. Therefore, the AGB and AGC stocks of seedlings were both 0 ton · ha^{-1}. Mature mangroves (with DBH ≥5 cm) were compared in terms of their AGB and AGC stocks based on species composition (Figure 5a, b). Overall, species composition significantly influenced AGB and AGC stocks in the Banlaem mangrove forest. The coexistence of *A. marina* and *Rhizophora* spp. resulted in high AGB (43.4–180; mean ± SD: 108 ± 33.5 ton · ha^{-1}) and AGC (21.7–89.9; 53.8 ± 16.7 ton · ha^{-1}) stocks. These values were significantly higher than those recorded in *A. marina*-only plots (t_{34} = -6.68, P< 0.001), which had an AGB of 3.2–102 (38.6±27.9) ton · ha^{-1}and AGC stock of 1.6–51.0 (19.3±14.0) ton · ha^{-1}. The higher wood density of the *Rhizophora* spp. (*R. mucronata* = 0.82 g/cm^3; *R. apiculata* = 0.85 g/cm^3) likely contributes to the higher AGB compared to the lower wood density of the *A. marina* (0.65 g/cm^3).

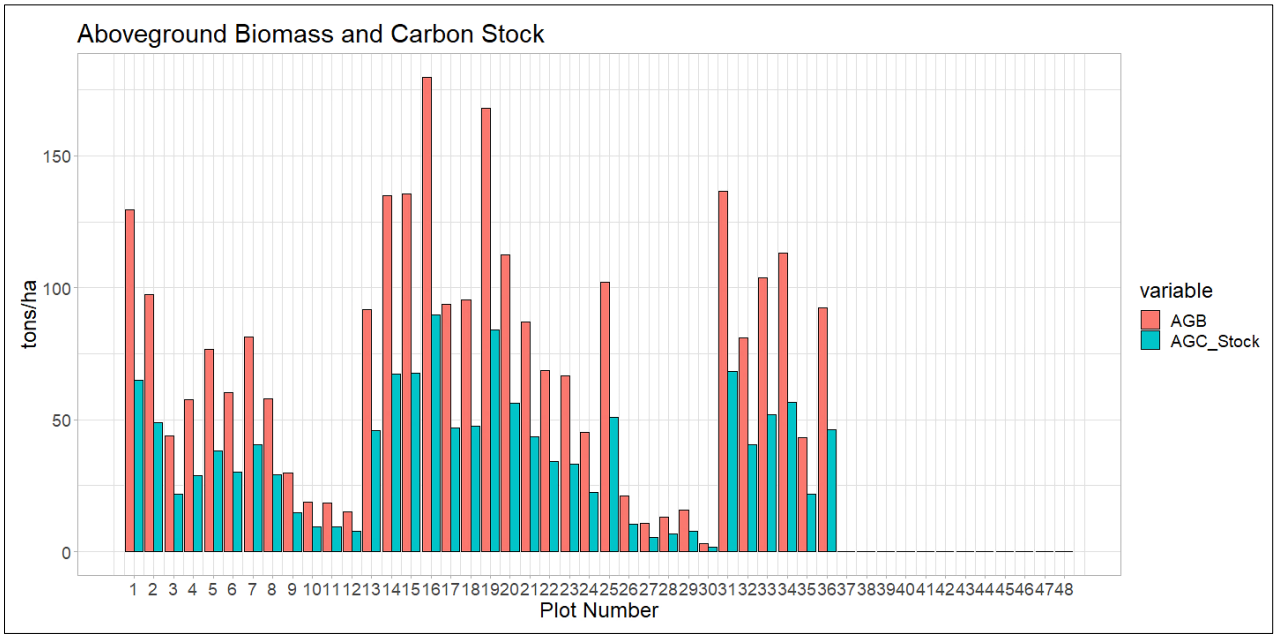

Figure 4. The AGB (red bar) and AGC (green bar) stocks in each study plot of the Banlaem mangrove forest

3.2. Model Development and Validation

Regression models for estimating mangrove AGB and AGC were developed using UAV and satellite data, various vegetation indices, and CHM data (Table 4). Overall, combining multiple indices (NDVI, SAVI, GNDVI) and CHM significantly improved model accuracy (R^2: 0.147–0.729; *RMSE*: 22.0–29.0 ton · ha^{-1}) compared to single-index models (R^2: 0.070–0.177; *RMSE*: 38.3–40.7 ton · ha^{-1}). For the UAV data, NDVI was the most effective single index (R^2: 0.108; *RMSE*: 32.2 ton · ha^{-1}). For Sentinel-2 data, NDVI, SAVI, and GNDVI showed equal performance as the most effective single indices (R^2: 0.177; *RMSE*: 38.3 ton · ha^{-1}). For Landsat-8, NDVI was the most effective single index (R^2: 0.108; *RMSE*: 39.9 ton · ha^{-1}). Additionally, the use of the vertical variable (CHM) resulted in lower accuracy compared to the VIs. NDVI was the most effective single variable for estimating mangrove AGB across all tested platforms. However, this study suggests incorporating multiple variables for AGB prediction in the Banlaem mangrove forest, as they provided the highest accuracy across all tested platforms.

The type of equipment also influenced the accuracy of the AGB models (Figure 6). Scatter plots generated from the best model for each platform showed that the model achieved the highest accuracy, no. 14 (R^2 = 0.729, *RMSE* = 22.0 ton*ha¹, $P < 0.001$), which combined vegetation indices (NDVI, SAVI, and GNDVI) from both Landsat-8 and Sentinel-2 with CHM data from the UAV. Among the single-platform models, the UAV proved to be the most effective. The UAV achieved the highest accuracy among single-platform models in model no.5 (R^2 = 0.577, *RMSE* = 27.5 ton · ha^{-1}, $P< 0.001$), followed by the Sentinel-2 in model no.9 (R^2 = 0.529, *RMSE* = 29.0 ton · ha^{-1}, $P< 0.001$), and Landsat-8 in model no.13 (R^2 = 0.174, *RMSE* = 38.0 ton.ha^{-1}, $P< 0.05$). Overall, integrating multiple platforms and variables significantly improved the accuracy of the mangrove above-ground biomass (AGB) model in the Banlaem mangrove forest. In addition, residual plots were constructed to confirm the linearity of the models developed in this study (Figure 7). The most accurate models for all the tested platforms (UAV, Sentinel-2, Landsat-8, and the integrated system) showed that residuals were randomly distributed around the horizontal line (y-axis = 0). Therefore, these findings suggest that a linear relationship between the independent and dependent variables is sufficient for this study, thereby eliminating the need to explore non-linear modeling approaches.

Table 3. The ground data and biodiversity indices in the Banlaem mangrove forest

Mature Trees									
Plot	Species Occurrence			Tree Density (No.* ha-1)	Mean DBH (cm)	BA ($m^2.ha^{-1}$)	Diversity Index		
	R. mucronata	*R. apiculata*	*A. marina*				1-D	H	J
1	✓	×	✓	4,355	7.61	21.42	0.49	0.69	0.99
2	✓	×	✓	2,535	8.64	16.16	0.14	0.27	0.39
3	×	×	✓	1,690	7.61	8.02	0.00	0.00	0.00
4	×	×	✓	2,015	7.83	10.28	0.00	0.00	0.00
5	×	×	✓	3,250	7.28	14.34	0.00	0.00	0.00
6	×	×	✓	3,770	8.07	12.08	0.00	0.00	0.00
7	✓	×	✓	2,340	7.17	13.72	0.24	0.34	0.49
8	×	×	✓	2,340	7.17	10.81	0.00	0.00	0.00
9	×	×	✓	1,300	6.27	6.01	0.00	0.00	0.00
10	×	×	✓	845	6.55	3.65	0.00	0.00	0.00
11	×	×	✓	780	6.79	3.27	0.00	0.00	0.00
12	×	×	✓	1,365	6.85	5.51	0.00	0.00	0.00
13	✓	×	✓	2,665	7.89	13.34	0.05	0.11	0.17
14	✓	×	✓	3,055	8.58	19.01	0.12	0.24	0.34
15	✓	×	✓	2,340	9.44	17.85	0.15	0.29	0.41
16	✓	×	✓	2,015	11.62	22.33	0.27	0.44	0.64
17	✓	×	✓	1,430	10.41	13.17	0.50	0.69	1.00
18	✓	×	✓	1,950	9.26	14.43	0.44	0.64	0.92
19	✓	×	✓	3,965	8.57	23.64	0.06	0.14	0.21
20	✓	×	✓	2,795	8.53	16.68	0.30	0.48	0.69
21	✓	×	✓	2,210	8.35	13.34	0.46	0.65	0.94
22	✓	×	✓	1,690	9.13	11.48	0.20	0.36	0.52
23	×	×	✓	2,080	8.26	11.69	0.00	0.00	0.00
24	×	×	✓	2,145	7.15	8.67	0.00	0.00	0.00
25	×	×	✓	1,690	10.50	15.72	0.00	0.00	0.00
26	×	×	✓	455	9.71	3.48	0.00	0.00	0.00
27	×	×	✓	260	9.12	1.37	0.00	0.00	0.00
28	×	×	✓	455	7.98	2.37	0.00	0.00	0.00
29	×	×	✓	390	8.70	2.58	0.00	0.00	0.00
30	×	×	✓	130	7.64	0.60	0.00	0.00	0.00
31	✓	×	✓	3,315	8.52	19.31	0.04	0.10	0.14
32	✓	×	✓	1,755	8.83	11.74	0.35	0.53	0.76
33	✓	×	✓	2,210	9.02	15.15	0.42	0.61	0.87
34	✓	✓	✓	1,820	10.53	17.06	0.30	0.56	0.81
35	✓	✓	✓	1,430	8.08	7.60	0.24	0.49	0.70
36	✓	×	✓	1,690	9.89	12.64	0.50	0.69	1.00
	Mean			**1,959**	**8.43**	**11.68**	**0.15**	**0.23**	**0.33**
	SD			**1,034.31**	**1.23**	**6.20**	**0.18**	**0.27**	**0.38**

Seedlings									
Plot	Species Occurrence			Tree Density (No.* ha-1)	Mean DBH (cm)	BA (m^2. ha^{-1})	Diversity Index		
	R. mucronata	*R. apiculata*	*A. marina*				1-D	H	J
37	✓	×	×	10,000	0.00	0.00	0.00	0.00	0.00
38	✓	×	×	10,000	0.00	0.00	0.00	0.00	0.00
39	✓	×	×	20,000	0.00	0.00	0.00	0.00	0.00
40	×	×	✓	10,000	0.00	0.00	0.00	0.00	0.00
41	✓	×	×	10,000	0.00	0.00	0.00	0.00	0.00
42	✓	×	×	10,000	0.00	0.00	0.00	0.00	0.00
43	✓	×	×	10,000	0.00	0.00	0.00	0.00	0.00
44	✓	×	×	10,000	0.00	0.00	0.00	0.00	0.00
45	×	×	✓	10,000	0.00	0.00	0.00	0.00	0.00
46	✓	×	×	20,000	0.00	0.00	0.00	0.00	0.00
47	✓	×	×	10,000	0.00	0.00	0.00	0.00	0.00
48	✓	×	×	10,000	0.00	0.00	0.00	0.00	0.00
Mean				**11,667**	**0.00**	**0.00**	**0.00**	**0.00**	**0.00**
SD				**3,892.49**	**0.00**	**0.00**	**0.00**	**0.00**	**0.00**

Table 4. The AGB model development in this study

Equipment	Variable	Model No.	Equation	*R*	R^2	*p*-value	*RMSE* (ton.ha^{-1})
UAV	NDVI	1	AGB = 58.5+51.7(NDVI)	0.329	0.108	0.08	39.2
	SAVI	2	AGB = 58.5+34.5(SAVI)	0.329	0.108	0.08	39.9
	GNDVI	3	AGB = 60.8+46.4(GNDVI)	0.301	0.091	0.11	40.3
	CHM	4	AGB = 35.05+5.68(CHM)	0.265	0.070	0.16	40.7
	NDVI, SAVI, GNDVI, CHM	5	AGB = -51.68+5.53 (CHM) -40,122.32 (NDVI)+ 28,315.69 (SAVI) -2,185.20(GNDVI)	0.759	0.577	<0.001	27.5
Sentinel-2	NDVI	6	AGB = -200+518(NDVI)	0.420	0.177	<0.05	38.3
	SAVI	7	AGB = -200+345(SAVI)	0.420	0.177	<0.05	38.3
	GNDVI	8	AGB = -200+345(GNDVI)	0.420	0.177	<0.05	38.3
	NDVI, SAVI, GNDVI	9	AGB = -207+523,714(NDVI)- 351,237(SAVI)+4,084(GNDVI)	0.727	0.529	<0.001	29.0
Landsat-8	NDVI	10	AGB = 58.5+51.7(NDVI)	0.329	0.108	0.12	39.9
	SAVI	11	AGB = 219-318(SAVI)	0.292	0.085	0.12	40.4
	GNDVI	12	AGB = 223-545(GNDVI)	0.291	0.085	0.12	40.4
	NDVI, SAVI, GNDVI	13	AGB = 237-4.25×10^{-7}(NDVI)+ 2.83×10^{-7} (SAVI)-726 (GNDVI)	0.417	0.174	<0.05	38.4
Combination (UAV+Sentine l-2+Landsat-8)	All variables	14	AGB = 243.04+4.63(CHM)-41,111.90(UAV-NDVI) +28,836.37(UAV-SAVI)- 2,086.54(UAV-GNDVI)- 1.23×10^{-7}(Sentinel2-NDVI) +8.19×10^{6} (Sentinel2-SAVI) + 2.33×10^{8}(Landsat8-NDVI)- 1.55×10^{-8} (Landsat8-SAVI)+2,098.77(Landsat8-GNDVI)	0.854	0.729	<0.001	22.0

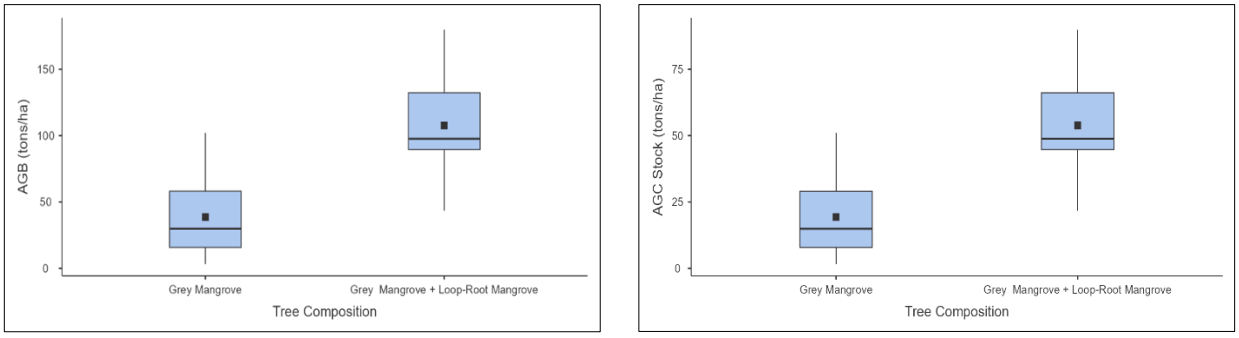

(a) (b)

Figure 5. The boxplots of (a) the AGB (tons/ha) and (b) AGC stock (tons/ha) in the Banlaem mangrove are based on tree composition

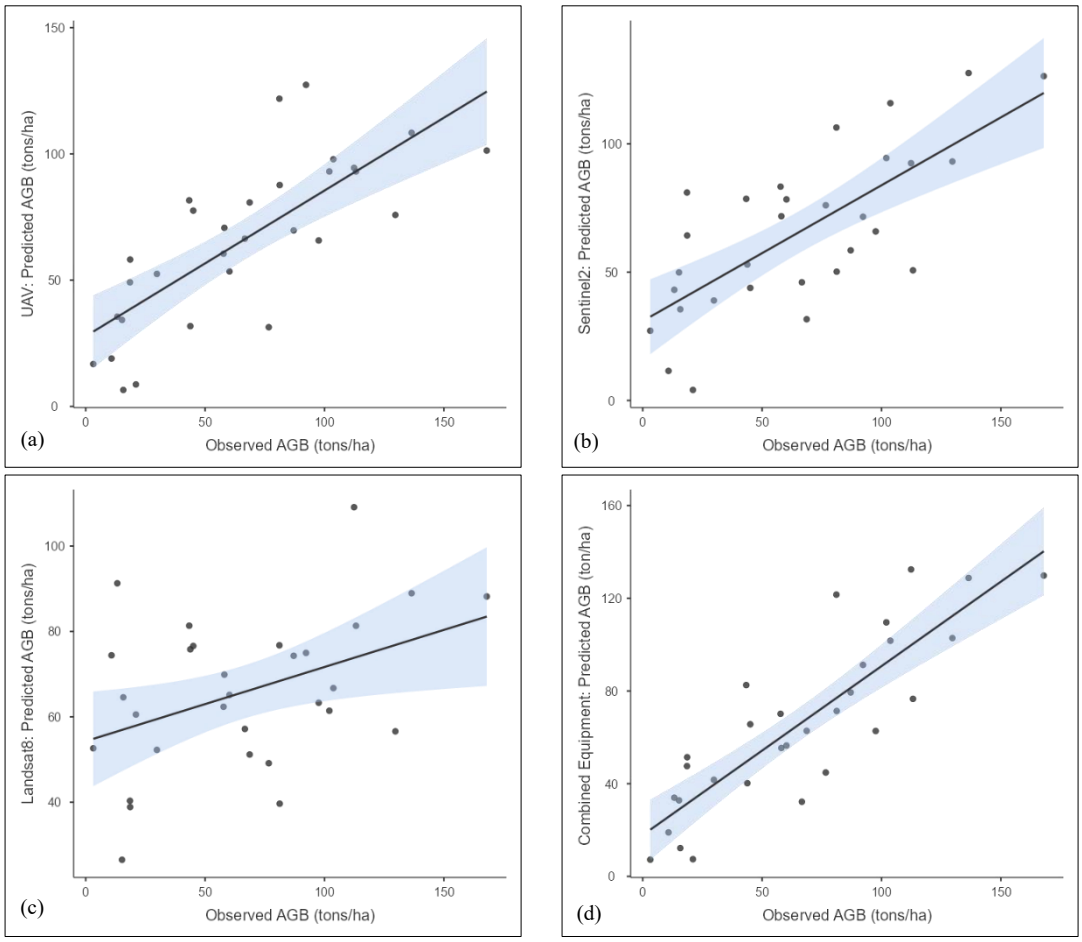

Figure 6. The most accurate AGB model in each equipment: (a) UAV, (b) Sentinel-2, (c) Landsat-8, and (d) combination (UAV+Sentinel-2+Landsat-8)

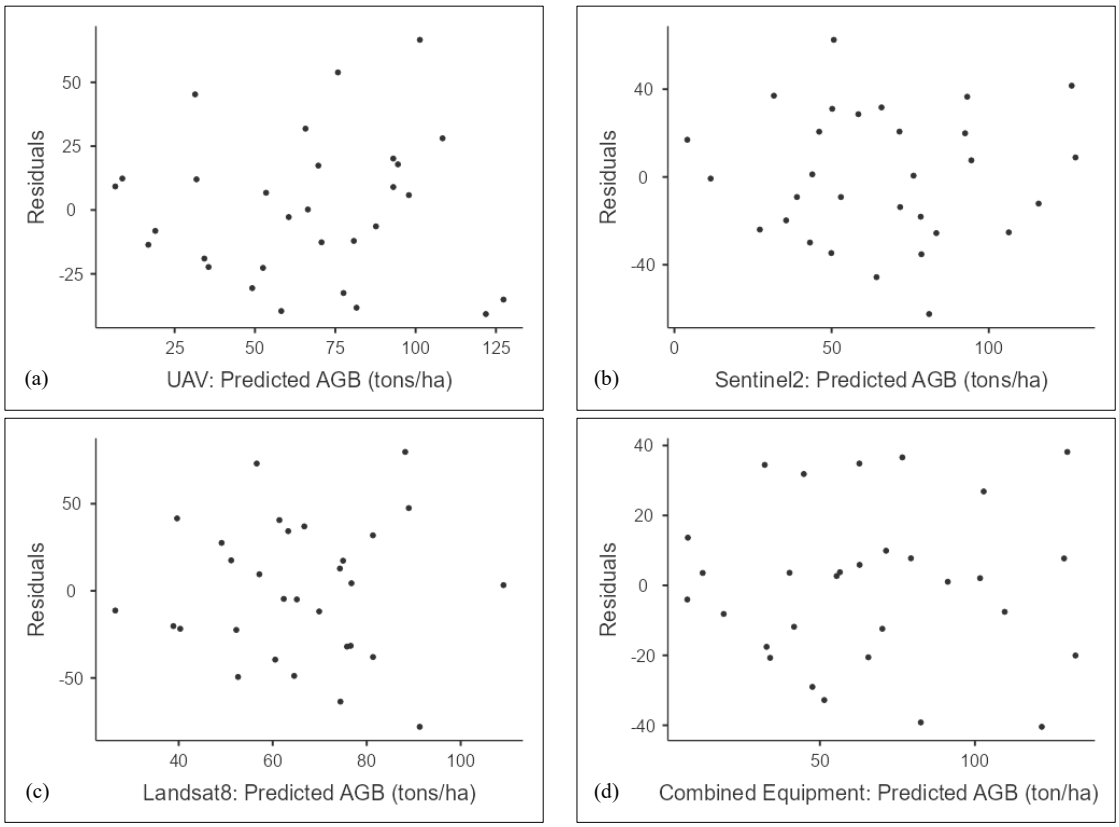

Figure 7. Residual plots of the AGB models in the most accurate AGB model in each equipment: (a) UAV, (b) Sentinel-2, (c) Landsat-8, and (d) combination (UAV+Sentinel-2+Landsat-8)

4. Discussion

4.1. Mangrove Biomass and Carbon Stock

This study provides the first assessment of the AGB, AGC stock, and diversity in the Banlaem mangrove forest in Nakhon Si Thammarat, southern Thailand. With its species richness (richness = 3), the findings indicate a relatively low diversity among mangrove tree species compared to other studies conducted in planted mangrove ecosystems within Thailand. *R. mucronata* was the only species planted in Banlaem, while it is evident that propagules of other species were dispersed by the tidal currents [19]. A survey of the Ranong Biosphere Reserve (RBR) in Ranong province, southern Thailand, revealed the presence of four mangrove species, belonging to three genera: *Rhizophora*, *Bruguiera*, and *Ceriops* [14]. Mangrove DBH was significantly higher in the RBR (15.12 ± 7.34 cm) than in the Banlaem forest (6.32 ± 3.84 cm), in this study. A lower AGB range in the Banlaem mangrove forest (0–179.78 ton · ha^{-1}) likely resulted in a reduced AGC stock when contrasted with the RBR, where AGB ranged from 117.78 to 336.41 ton · ha^{-1}. Notably, the lowest AGB recorded in this study (AGB = 0 ton · ha^{-1}) was observed in mangrove seedlings, while the highest AGB in the RBR study (AGB = 336.41 ton · ha^{-1}) was found in the mixed species conservation forest area [14]. In another study, mangrove diversity exhibited a positive correlation with both biomass and carbon storage, and the evaluation of carbon storage was typically conducted using an allometric equation based on tree DBH [34]. Therefore, the small diameter and low diversity (1-D = 0.11±0.17, H = 0.17±0.25, and J = 0.25±0.36) in this Banlaem mangrove forest study contributed to their reduced carbon storage capacity. Research conducted at the Sirinart Rajini Ecosystem Learning Center in Prachuap Khiri Khan Province, southern Thailand, revealed that the mangrove forest exhibited a species richness six times greater than that observed in Banlaem. However, the AGB in this location ranged from 0 to 159.63 ton · ha^{-1} [15], which is slightly lower than that recorded in the mangrove forest of Banlaem.

This suggests species richness alone cannot predict the AGB and AGC stock in mangrove forests. Several additional factors can influence mangrove biomass, such as latitude, tidal range, and heavy metal pollution [35]. Future studies could examine the effects of additional factors influencing biomass and carbon stock in the Banlaem mangrove, such as tidal range, metal pollution, and other factors. This study also identified that the mangrove composition influences the AGB and AGC stocks in the Banlaem mangrove forest (Figure 5). The presence of *A. marina* and *Rhizophora* spp. in the composition leads to a higher AGB than plots dominated by a single species of *A. marina*. This finding aligns with previous studies that have shown *Rhizophora* spp. generally to have a greater biomass compared to *Avicennia* spp. [15], and that mixed-species plots exhibit higher biomass than those dominated by a single species [14]. It could be due to the higher wood density *of R. mucronata* and *R. apiculata,* which results in higher biomass compared with *A. marina* in this study.

4.2. Mangrove AGB Model

For the model validation in this study, it was found that the combination of the tested VIs and equipment contributed to the effectiveness of mangrove biomass prediction. The combined VIs (including CHM from the UAV) exhibited the highest accuracy with each type of equipment. The most effective tools (Table 4; Figure 6), in order, were the combined equipment (model no.14), UAV (model no.5), Sentinel-2 (model no. 9), and Landsat-8 (model no. 13). Compared to previous research in Thailand, this study is the first to employ UAVs, Landsat-8, and Sentinel-2 imagery with VIs for estimating mangrove biomass and carbon storage. In Ranong province, southern Thailand, a research study utilized medium-resolution (ASTER) and high-resolution (GeoEye-1) satellite data, in conjunction with machine learning techniques, to model mangrove biomass [13]. Their study found that the optimal AGB model achieved an R^2 value of 0.66. [13]. Compared to their research, the combined model (model no. 14) applied to the Banlaem mangrove in this study demonstrated slightly better performance, achieving an R^2 value of 0.73. Similarly, the use of the two satellites (Sentinel-2 and Landsat-8), along with UAVs equipped with VIs and the height model, has been reported in other Southeast Asian countries. In Quang Ninh Province, Vietnam, the model utilizing NDVI and tree height data from UAV demonstrated high accuracy (R^2 = 0.831, $RMSE$ = 0.040 ton · ha^{-1}) in estimating the mangrove AGB [17]. In contrast to other studies, which indicated that Landsat-8 (R^2 values ranging from 0.86 to 0.94) and Sentinel-2 (R^2 values ranging from 0.97 to 0.99) were highly effective in estimating mangrove AGB [7, 36]. Additionally, in Komodo National Park, Indonesia, multi-source RS data combined with machine learning techniques were utilized to estimate mangrove AGB, with the optimal model achieving an R^2 value of 0.76 [18]. Hence, the findings of this study align with previous research [36], demonstrating that the combination of the tested VIs enhances the model's effectiveness. Various factors, such as cloud-cover percentage, date consistency, and mangrove characteristics, may affect the model's accuracy. Besides these, the uneven-aged trees or species composition can lead to a low approach accuracy [37].

Certain limitations arose in this study. Some study plots (plots 13-18) were not assessed for their VIs from the UAV due to their location within a flight restriction zone (no-fly zone) near an airport. Consequently, these plots were excluded from the model assessment in this study. Cloud cover influenced satellite image selection for multispectral RS data, resulting in imagery dates that may not align with the fieldwork period. Furthermore, for the UAV data, the

height model exhibited a low correlation with the AGB, with an R^2 value of 0.070. The dense canopy of the mangrove may have interfered with the signal from the UAV. To enhance model accuracy, future studies should explore the use of LiDAR, given its proven ability to accurately assess mangrove vertical structure [38].

The modeling approach developed in this study can be applied to other mangrove ecosystems. A study was conducted at the Mangrove Forest Resource Development and Learning Center 2 in Nakhon Si Thammarat [16], revealing a higher species diversity with six mangrove species identified. Despite this diversity, *A. marina* and *Rhizophora* species were found to be dominant. The research relied on field-based methods and reported a carbon stock of 29.69 tons ha-1, compared to 28.15 ± 25.90 tons ha-1 in Banlaem. The similarities in dominant species and carbon storage capacity between the two mangrove sites suggest that the modeling approach developed in this study could be effectively applied to the Mangrove Forest Resource Development and Learning Center 2 for monitoring. This would help address challenges associated with field data collection.

It is advisable to apply the modeling approach used in this study to mangrove areas with similar characteristics. The Banlaem mangrove forest, for example, displays a clear zonation pattern, with *A. marina* dominating the interior and few *Rhizophora* species found along the outer edge. Some studies have been conducted in areas of very high biodiversity, compared to the Banlaem mangroves [39]. Specific models—linear, non-linear, and those incorporating mangrove height—were developed based on the distinct characteristics of each mangrove type [5, 7, 39]. Additionally, the choice of models may vary depending on the scale of the study.

4.3. Implications

To facilitate a comprehensive carbon assessment in the Banlaem mangrove forest, it is recommended that impact assessments be initiated, monitoring and evaluation plans be developed, and community engagement be fostered. The findings of this study highlight the utility of multispectral data in accurately estimating mangrove biomass and carbon stock. A reproducible framework for carbon stock assessment in the Banlaem mangrove forest and comparable tropical mangrove ecosystems in Thailand is provided by the suggested methodological approach and mathematical models, notably model 14 (Table 4). The findings of this study contribute to Thailand's national emission reduction target work, which include achieving carbon neutrality by 2050 and net-zero greenhouse gas (GHG) emissions by 2065. To align with these goals, Thailand has revised its Nationally Determined Contributions (NDC) strategy, raising the GHG emissions reduction target to 40% by 2030, a significant increase from the previous 25% [40]. Ultimately, given the voluntary market mechanism in Thailand, this study provides comprehensive support to land managers in making informed decisions about harvesting, tree planting, and habitat conservation in this promising area, thereby fostering community engagement in sustainable management and carbon offset initiatives. Notably, for the Banlaem community, which sees around 300-400 tourists and students visiting the Banlaem mangrove forest each month to plant mangrove trees [19], this study could help the local community recognize the increasing importance of carbon storage in mangroves. It would also enhance the collection of various statistical data to assess the changes resulting from planting mangroves, particularly in reducing greenhouse gases. Additionally, this study found that combining grey and loop-root mangroves in this area yields a higher carbon stock than grey mangroves alone (Figure 5). This finding will be helpful to authorities in formulating the mangrove plantation plan and management strategies for the planted Banlaem mangrove forest, supporting blue carbon management.

To integrate the findings of this study into the policy frameworks for the Banlaem community, we recommend applying this assessment method, along with the associated techniques, to the Thailand Voluntary Emission Reduction (T-VER) program. This program serves as a mechanism for reducing greenhouse gas (GHG) emissions, permitting the use of remote sensing and alternative techniques, subject to approval by the Thailand Greenhouse Gas Management Organization (TGO) [41]. Alternatively, we suggest incorporating the Low Emission Support Scheme (LESS), which promotes the development of activity models aimed at raising awareness about greenhouse gas (GHG) reduction. The scheme also recognizes individuals or groups who contribute positively by awarding certificates of honor [42]. This not only supports GHG emission reduction but also fosters environmental awareness and promotes ecotourism within the community.

5. Conclusion

This study represents a significant advancement in understanding and managing mangrove carbon stocks, particularly within the Banlaem region. This study assessed the AGB and AGC stocks in the Banlaem mangroves and developed a technique for generating an AGB prediction model in this mangrove ecosystem. Three mangrove species were observed at the study site, reflecting low biodiversity in this mangrove area. In addition to the planted species (*R. mucronata*), *A. marin*a and *R. apiculata* were also found. Overall, the AGB and AGC stocks were relatively high, particularly in areas where *A. marina* and *R. mucronata* coexisted. To develop the AGB model for the Banlaem mangroves, this study demonstrated that using vegetation indices (NDVI, SAVI, and GNDVI) integrated with the vertical model (CHM) significantly improved AGB prediction. Integrating data from two satellites with UAV imagery

achieved the highest accuracy in the prediction, with an R^2 value of 0.73 and an *RMSE* of 22.0 tons · ha^{-1}. Therefore, the model applies to the Banlaem mangroves. This is the first study to quantify carbon stock in this mangrove forest and propose a novel approach to estimate mangrove AGB. The findings highlight the effectiveness of integrating multiple data sources and variables to enhance model accuracy. Ultimately, this study provides essential data on mangrove carbon stock to the Banlaem community and introduces a method for its measurement, offering a foundation for assessment, monitoring, and community engagement in mangrove carbon evaluation. The evaluation supports Thailand's carbon neutrality and greenhouse gas (GHG) reduction goals under its Nationally Determined Contribution (NDC) to the Paris Agreement. This approach could be implemented through voluntary carbon markets, such as the Thailand Voluntary Emission Reduction Program (T-VER).

6. Declarations

6.1. Author Contributions

Conceptualization, S.P. and S.C.; methodology, S.P. and S.C.; formal analysis, S.P.; investigation, S.P.; resources, K.J. and M.J.; data curation, S.P. and W.S.; writing—original draft preparation, S.P.; writing—review and editing, K.J., M.J., E.S., and S.C.; visualization, S.P. and W.S.; supervision, K.J. and M.J.; funding acquisition, S.C. All authors have read and agreed to the published version of the manuscript.

6.2. Data Availability Statement

The data presented in this study are available on request from the corresponding author.

6.3. Funding

The Development and Promotion of Science and Technology Talents Project (DPST), the Thai Government Scholarship, and the Suranaree University of Technology generously funded this project.

6.4. Acknowledgments

This project is conducted within the Reinventing Project for Enhancing Thai Universities into International Education, a project of the Ministry of Higher Education, Science, Research, and Innovation. The researchers would like to express our sincere gratitude to the Development and Promotion of Science and Technology Talents Project (DPST), the Thai Government Scholarship, the Center of Excellence for Ecoinformatics, Research and Innovation Institute of Excellence, Walailak University, and the School of Biology, Institute of Science, Suranaree University of Technology, for their invaluable facility and support throughout the project.

6.5. Institutional Review Board Statement

Not applicable.

6.6. Informed Consent Statement

Not applicable.

6.7. Declaration of Competing Interest

The authors declare that there are no conflicts of interest concerning the publication of this manuscript. Furthermore, all ethical considerations, including plagiarism, informed consent, misconduct, data fabrication and/or falsification, double publication and/or submission, and redundancies have been completely observed by the authors.

7. References

[1] Choudhary, B., Dhar, V., & Pawase, A. S. (2024). Blue carbon and the role of mangroves in carbon sequestration: Its mechanisms, estimation, human impacts and conservation strategies for economic incentives. Journal of Sea Research, 199, 102504. doi:10.1016/j.seares.2024.102504.

[2] Alongi, D. M. (2014). Carbon cycling and storage in mangrove forests. Annual Review of Marine Science, 6, 195–219. doi:10.1146/annurev-marine-010213-135020.

[3] Paramanik, S., Varghese, R., Behera, M. D., Barnwal, S., Behera, S. K., & Bhattyacharya, B. K. (2022). Photosynthetic variables estimation in a mangrove forest. Advances in Remote Sensing for Forest Monitoring, 126–149. doi:10.1002/9781119788157.ch6.

[4] Dutta Roy, A., Pitumpe Arachchige, P. S., Watt, M. S., Kale, A., Davies, M., Heng, J. E., Daneil, R., Galgamuwa, G. A. P., Moussa, L. G., Timsina, K., Ewane, E. B., Rogers, K., Hendy, I., Edwards-Jones, A., de-Miguel, S., Burt, J. A., Ali, T., Sidik, F., Abdullah, M., … Mohan, M. (2024). Remote sensing-based mangrove blue carbon assessment in the Asia-Pacific: A systematic review. Science of the Total Environment, 938, 173270. doi:10.1016/j.scitotenv.2024.173270.

[5] Mariano Neto, M., da Silva, J. B., & de Brito, H. C. (2024). Carbon stock estimation in a Brazilian mangrove using optical satellite data. Environmental Monitoring and Assessment, 196(1), 9. doi:10.1007/s10661-023-12151-3.

[6] Wang, D., Wan, B., Liu, J., Su, Y., Guo, Q., Qiu, P., & Wu, X. (2020). Estimating aboveground biomass of the mangrove forests on northeast Hainan Island in China using an upscaling method from field plots, UAV-LiDAR data and Sentinel-2 imagery. International Journal of Applied Earth Observation and Geoinformation, 85, 101986. doi:10.1016/j.jag.2019.101986.

[7] Nguyen, H. H., & Nguyen, T. T. H. (2021). Above-ground biomass estimation models of mangrove forests based on remote sensing and field-surveyed data: Implications for C-PFES implementation in Quang Ninh Province, Vietnam. Regional Studies in Marine Science, 48, 101985. doi:10.1016/j.rsma.2021.101985.

[8] Shangari, T. A., Shams, V., Azari, B., Shamshirdar, F., Baltes, J., & Sadeghnejad, S. (2017). Inter-humanoid robot interaction with emphasis on detection: a comparison study – ADDENDUM. The Knowledge Engineering Review, 32, 14. doi:10.1017/s0269888917000078.

[9] Tassi, A., & Vizzari, M. (2020). Object-oriented lulc classification in google earth engine combining snic, glcm, and machine learning algorithms. Remote Sensing, 12(22), 1–17. doi:10.3390/rs12223776.

[10] Rina, S., Ying, H., Shan, Y., Du, W., Liu, Y., Li, R., & Deng, D. (2023). Application of Machine Learning to Tree Species Classification Using Active and Passive Remote Sensing: A Case Study of the Duraer Forestry Zone. Remote Sensing, 15(10), 10. doi:10.3390/rs15102596.

[11] Farzanmanesh, R., Khoshelham, K., Volkova, L., Thomas, S., Ravelonjatovo, J., & Weston, C. J. (2024). Quantifying Mangrove aboveground biomass changes: Analysis of conservation impact in blue forests projects using sentinel-2 satellite imagery. Forest Ecology and Management, 561, 121920. doi:10.1016/j.foreco.2024.121920.

[12] Bajaj, M., Sasaki, N., Tsusaka, T. W., Venkatappa, M., Abe, I., & Shrestha, R. P. (2024). Assessing changes in mangrove forest cover and carbon stocks in the Lower Mekong Region using Google Earth Engine. Innovation and Green Development, 3(3), 100140. doi:10.1016/j.igd.2024.100140.

[13] Jachowski, N. R. A., Quak, M. S. Y., Friess, D. A., Duangnamon, D., Webb, E. L., & Ziegler, A. D. (2013). Mangrove biomass estimation in Southwest Thailand using machine learning. Applied Geography, 45, 311–321. doi:10.1016/j.apgeog.2013.09.024.

[14] Macintosh, D. J., & Ashton, E. C. (2023). Growth and carbon stocks in four mangrove species planted on a former charcoal concession site in Ranong, Thailand. Carbon Footprints, 2(3), 14. doi:10.20517/cf.2023.26.

[15] Sribut, S., Sunthornhao, P., & Diloksumpun, S. (2020). Valuation of Carbon Stock and Utilization of Non-timber Forest Products at the Sirinart Rajini Ecosystem Learning Center, Prachuap Khiri Khan Province. Thai Journal of Forestry, 39(2), 41–51.

[16] Srimoh R., Markphan W., (2024). Carbon Stocks in Mangrove Forests at Mangrove Forest Learning and Development Center 2, Nakhon Si Thammarat. Srinakharinwirot University Journal of Sciences and Technology, 16(1), 251943.

[17] Ngo, D. T., Nguyen, H. D., Nguyen, K. Q., Dang, C. H., Nguyen, H. H. V., Dang, N. T., & Pham, T. V. (2023). Application of multispectral UAV to estimate mangrove biomass in Vietnam: A case study in Dong Rui commune, Quang Ninh Province. One Ecosystem, 8, 103760. doi:10.3897/oneeco.8.e103760.

[18] Rijal, S. S., Pham, T. D., Noer'Aulia, S., Putera, M. I., & Saintilan, N. (2023). Mapping Mangrove Above-Ground Carbon Using Multi-Source Remote Sensing Data and Machine Learning Approach in Loh Buaya, Komodo National Park, Indonesia. Forests, 14(1), 94. doi:10.3390/f14010094.

[19] Jaroensutasinee, K., Jaroensutasinee, M., Detrattanawichai, S., & Sparrow, E. (2024). Factors Affecting Population Density and Mound Distribution of Mud Lobsters, Thalassina spp. Emerging Science Journal, 8(1), 169–179. doi:10.28991/ESJ-2024-08-01-012.

[20] World Bank. (2023). World Bank Climate Change Knowledge Portal: Bangladesh Overview. World Bank, Washington, D.C., United States. Available online: https://climateknowledgeportal.worldbank.org/ (accessed on May 2025).

[21] Kauffman, J. B., & Donato, D. C. (2012). Protocols for the measurement, monitoring, and reporting of structure, biomass, and carbon stocks in mangrove forests. Volume 86, CIFOR Bogor, Indonesia.

[22] Zarawie, T. T., Suratman, M. N., Jaafar, J., Hasmadi, I. M., & Abu, F. (2015). Field assessment of aboveground biomass (AGB) of mangrove stands in Merbok, Malaysia. Malaysian Applied Biology, 44(3), 81–86.

[23] DMCR. (2012). Mangrove plant species in Thailand. Department of Marine and Coastal Resources, Thailand. Available online: https://www.dmcr.go.th/detailLib/407 (accessed on May 2025).

[24] Komiyama, A., Poungparn, S., & Kato, S. (2005). Common allometric equations for estimating the tree weight of mangroves. Journal of Tropical Ecology, 21(4), 471–477. doi:10.1017/S0266467405002476.

[25] Zanne, A. E., Lopez-Gonzalez, G., Coomes, D. A., Ilic, J., Jansen, S., Lewis, S. L., Miller, R. B., Swenson, N. G., Wiemann, M. C., Chave, J., Zanne, A. E., Lopez-Gonzalez, G., Coomes, D. A., Ilic, J., Jansen, S., Lewis, S. L., Miller, R. B., Swenson, N. G., Wiemann, M. C., & Chave, J. (2009). Global Wood Density Database [Dataset]. Dryad Digital Repository. doi:10.5061/DRYAD.234/1.

[26] IPCC. (2006). 2006 IPCC Guidelines for National Greenhouse Gas Inventories. IPCC — Intergovernmental Panel on Climate Change, Geneva, Switzerland. Available online: https://www.ipcc-nggip.iges.or.jp/ public/2006gl/vol4.html (accessed on May 2025).

[27] Vinod, K., Koya, A. A., Kunhi Koya, V. A., Silpa, P. G., Asokan, P. K., Zacharia, P. U., & Joshi, K. K. (2018). Biomass and carbon stocks in mangrove stands of Kadalundi Estuarine Wetland, south-west coast of India. Indian Journal of Fisheries, 65(2), 89–99. doi:10.21077/ijf.2018.65.2.72473-11.

[28] Shannon, C. E. (1948). A Mathematical Theory of Communication. Bell System Technical Journal, 27(3), 379–423. doi:10.1002/j.1538-7305.1948.tb01338.x.

[29] Simpson, E. H. (1949). Measurement of diversity. Nature, 163(4148), 688. doi:10.1038/163688a0.

[30] Nasiri, V., Darvishsefat, A. A., Arefi, H., Pierrot-Deseilligny, M., Namiranian, M., & Le Bris, A. (2021). Unmanned aerial vehicles (Uav)-based canopy height modeling under leaf-on and leaf-off conditions for determining tree height and crown diameter (case study: Hyrcanian mixed forest). Canadian Journal of Forest Research, 51(7), 962–971. doi:10.1139/cjfr-2020-0125.

[31] Zaitunah, A., Samsuri, Ahmad, A., & Safitri, R. (2018). Normalized difference vegetation index (NDVI) analysis for land cover types using Landsat 8 OLI in Besitang watershed, Indonesia. 126, 012112. doi:10.1088/1755 1315/126/1/012112.

[32] Huete, A. R. (1988). A soil-adjusted vegetation index (SAVI). Remote Sensing of Environment, 25(3), 295–309. doi:10.1016/0034-4257(88)90106-X.

[33] Gitelson, A. A., Kaufman, Y. J., & Merzlyak, M. N. (1996). Use of a green channel in remote sensing of global vegetation from EOS- MODIS. Remote Sensing of Environment, 58(3), 289–298. doi:10.1016/S0034-4257(96)00072-7.

[34] Bai, J., Meng, Y., Gou, R., Lyu, J., Dai, Z., Diao, X., Zhang, H., Luo, Y., Zhu, X., & Lin, G. (2021). Mangrove diversity enhances plant biomass production and carbon storage in Hainan Island, China. Functional Ecology, 35(3), 774–786. doi:10.1111/1365-2435.13753.

[35] Wang, G., Singh, M., Wang, J., Xiao, L., & Guan, D. (2021). Effects of marine pollution, climate, and tidal range on biomass and sediment organic carbon in Chinese mangrove forests. Catena, 202, 105270. doi:10.1016/j.catena.2021.105270.

[36] Nguyen, H. H., Vu, H. D., & Röder, A. (2021). Estimation of above-ground mangrove biomass using landsat-8 data-derived vegetation indices: A case study in Quang Ninh province, Vietnam. Forest and Society, 5(2), 506–525. doi:10.24259/fs.v5i2.13755.

[37] Nguyen, L. D., Nguyen, C. T., Le, H. S., & Tran, B. Q. (2019). Mangrove mapping and above-ground biomass change detection using satellite images in coastal areas of Thai Binh Province, Vietnam. Forest and Society, 3(2), 248–261. doi:10.24259/fs.v3i2.7326.

[38] Tian, Y., Zhang, Q., Huang, H., Huang, Y., Tao, J., Zhou, G., Zhang, Y., Yang, Y., & Lin, J. (2022). Aboveground biomass of typical invasive mangroves and its distribution patterns using UAV-LiDAR data in a subtropical estuary: Maoling River estuary, Guangxi, China. Ecological Indicators, 136, 108694. doi:10.1016/j.ecolind.2022.108694.

[39] Wirasatriya, A., Pribadi, R., Iryanthony, S. B., Maslukah, L., Sugianto, D. N., Helmi, M., Ananta, R. R., Adi, N. S., Kepel, T. L., Ati, R. N. A., Kusumaningtyas, M. A., Suwa, R., Ray, R., Nakamura, T., & Nadaoka, K. (2022). Mangrove Above-Ground Biomass and Carbon Stock in the Karimunjawa-Kemujan Islands Estimated from Unmanned Aerial Vehicle-Imagery. Sustainability (Switzerland), 14(2), 706. doi:10.3390/su14020706.

[40] ONEP. (2022). Thailand's second updated nationally determined contribution. Natural Resources and Environmental Policy and Planning, Bangkok, Thailand. Available online: https://www.onep.go.th/en/ (accessed on May 2025).

[41] Thailand Greenhouse Gas Management Organization. (2025). Calculation for Carbon Sequestration in tree. GHG, Bangkok, Thailand. Available online: https://ghgreduction. tgo.or.th /th/tver-method/tver-tool/for-agr/item/3451-calculation-for-carbon-sequestration.html (accessed on May 2025).

[42] Thailand Greenhouse Gas Management Organization. (2016). What is LESS? GHG, Bangkok, Thailand. Available online: https://ghgreduction.tgo.or.th/th/about-less/about-less1.html (accessed on May 2025).